

Turning gaits and optimal undulatory gaits for a modular centipede-inspired millirobot

Katie L. Hoffman and Robert J. Wood

Abstract—Turning gaits and optimal undulatory straight-line gaits for a walking myriapod millirobot are presented. Simulation and experiments show that body undulations similar to those found in natural centipedes enhance straight-line locomotion via increased speeds and reduced cost of transport for myriapod millirobots with passively flexible bodies composed of a variety of segments. A simple turning strategy that uses an offset duty-cycle for the stance of contralateral legs was developed. Turning experiments for millirobots with 5-8 segments show that this can successfully be applied to millirobots with different numbers of legs. This millirobot, which is composed of 220 mg, two-legged segments, can be used to understand how to effectively implement characteristics of actual centipedes, such as body flexibility and many legs, into millirobots.

I. INTRODUCTION

Biological inspiration has been used to create small, agile ambulatory robots. Many of these are modeled after cockroaches, i.e. hexapods with rigid bodies, including DynaRoACH [1], DASH [2], and HAMR [3], which use the alternating tripod gait for locomotion. Another arthropod body morphology is that of the centipede, which have long, flexible bodies and up to 191 pairs of legs [4]. Unlike cockroaches, their gaits involve body undulations, or waves that travel along the body [5]. Often, the body curves around three groups of stance legs [6]. A centipede-inspired millirobot could have advantages over rigid body morphologies with the ability to morph to rough surfaces, smoothly transition from horizontal to vertical surfaces, and exhibit graceful degradation in locomotion performance when leg failures occur. The modular nature of a centipede millirobot allows any number of segments to be used to adapt the robot to different situations.

Straight-line locomotion of a 10-segment, 2.2 g centipede millirobot has been demonstrated at speeds up to 7 cm/s [7]. It was shown that body undulations, resulting from a passively compliant backbone, enhanced locomotion speed and cost of transport by increasing the step size of the robot due to the positive body rotation at the time of stance change, similar to that found in actual centipedes. The alternating gait, typically used by hexapods but not found in centipedes, resulted in reduced velocities due to negative body rotation.

The goal of this paper is to expand the idea of passive undulations to a centipede millirobot with an arbitrary number of segments. This involves answering the questions: Do locomotion enhancing undulations arise for millirobots

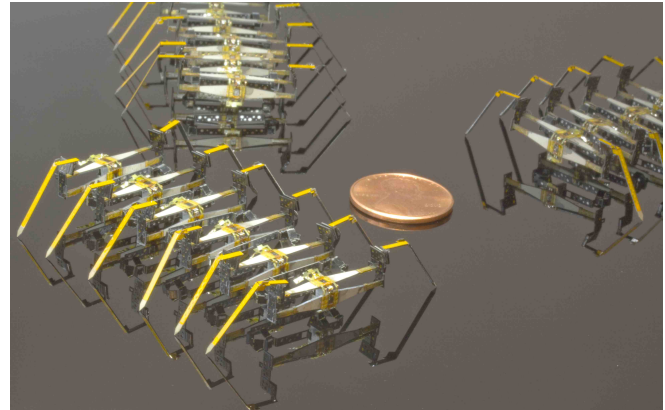


Fig. 1. Centipede millirobots with varying numbers of legs.

with only four or five segments? Also, what is the optimal phase difference between segments to attain the undulations that best increase the step size as a function of number of segments? How do the optimal gaits compare to those of actual centipedes in terms of phases between segments and body curvatures?

In addition to straight-line locomotion, methods for turning are also studied. Strategies used for cockroach millirobots, such as DynaRoACH, involve stiffening the middle leg on one side of the body to introduce an asymmetry into the alternating gait [1]. Turning by either altering the swing of contralateral legs or relative segment rotation was suggested for a larger centipede robot [8]. The goal of turning in this many-legged millirobot is to find a simple strategy that does not involve adding additional actuation and can be applied to any number of segments with coupled stance and swing degrees-of-freedom of contralateral legs.

The notional design of the millirobot, fabrication improvements over the previous version in [7], and brief overview of the dynamic model are presented in Sec. II. Optimal phases for straight-line locomotion are found in simulation and experiments in Sec. III as a function of the number of segments. Finally, a turning strategy is developed that involves changing the duty-cycle for stance between contralateral legs and tested experimentally in millirobots for 5, 6, 7, and 8 segments in Sec. IV. Given the similarities between this millirobot and actual centipedes, this platform may be used to study biological locomotion and how to effectively introduce compliance into myriapod robots at small scales.

The authors are with the School of Engineering and Applied Sciences and the Wyss Institute for Biologically Inspired Engineering, Harvard University, Cambridge, MA 02138 khoffman@fas.harvard.edu

II. NOTIONAL DESIGN, FABRICATION, AND MODELING

The centipede millirobot used to study myriapod locomotion is similar to that presented in [7] with improvements made to the design and fabrication process to reduce performance differences between individual segments. The millirobot is composed of individual two-legged segments (Fig. 2(b)) attached to adjacent segments by a passive, flexible backbone (Fig. 2(a)). Each segment has two actuated degrees of freedom (DOF): stance and swing of the legs, controlled by two piezoelectric bimorph actuators attached to two orthogonal four-bar mechanisms (Fig. 2(c)). While there are four actuators per segment to control the two legs, only two drive signals are used to control the stance and swing of the legs. By having opposite poling directions for the piezoelectric actuators controlling each leg and a shared drive signal as illustrated in (Fig. 2(d)), as one leg is being placed on the ground, the opposite leg on the same segment is being lifted. Similarly, for the swing DOF, as a torque is being applied to the stance leg, the swing leg on the opposite side of the segment is being reset in preparation for the next step. While this reduces the number of drive signals necessary, it does limit the number of techniques available for turning gaits, which rely on introducing asymmetries between contralateral legs. Most larger centipede-inspired robots have active rotational joints between segments [9],[10],[11], with a recent notable exception being [12]. Here, passive joints were chosen for the backbone to allow for natural system dynamics to create the locomotion-enhancing body undulations and eliminate the need for additional actuation. The backbone components connecting the segments have four passive rotational joints (flexures) and two passive linear joints (sarrus linkages), as shown in Fig. 2(a).

The layered fabrication process outlined in [13] was used to create this modular robot. A thin polymer film and fiber composites create a series of flexures and rigid links that form the mechanical components. Improvements to the previous design [7] were made to allow for batch fabrication of a many-legged millirobot and ensure consistent performance, including cascaded joints that allow for easy folding and alignment features on the transmission, actuators, flexible circuit, and backbone. Two wires per segment are used to attach the millirobot to an external power supply and controller.

To predict trends in locomotion across different numbers of segments, the dynamic model presented in more detail in [7] is used. This hybrid-dynamic model, which is illustrated in Fig. 3, is limited to the horizontal plane motion. In the horizontal plane, each segment has one actuated DOF and one passive DOF, assuming the stance feet act as pin joints with respect to ground, making this an underactuated system. These two DOFs are the horizontal plane leg angle, α , and the body angle, θ , with respect to a line perpendicular to the direction of motion. The Euler-Lagrange formulation and the system energies are used to derive the equations of

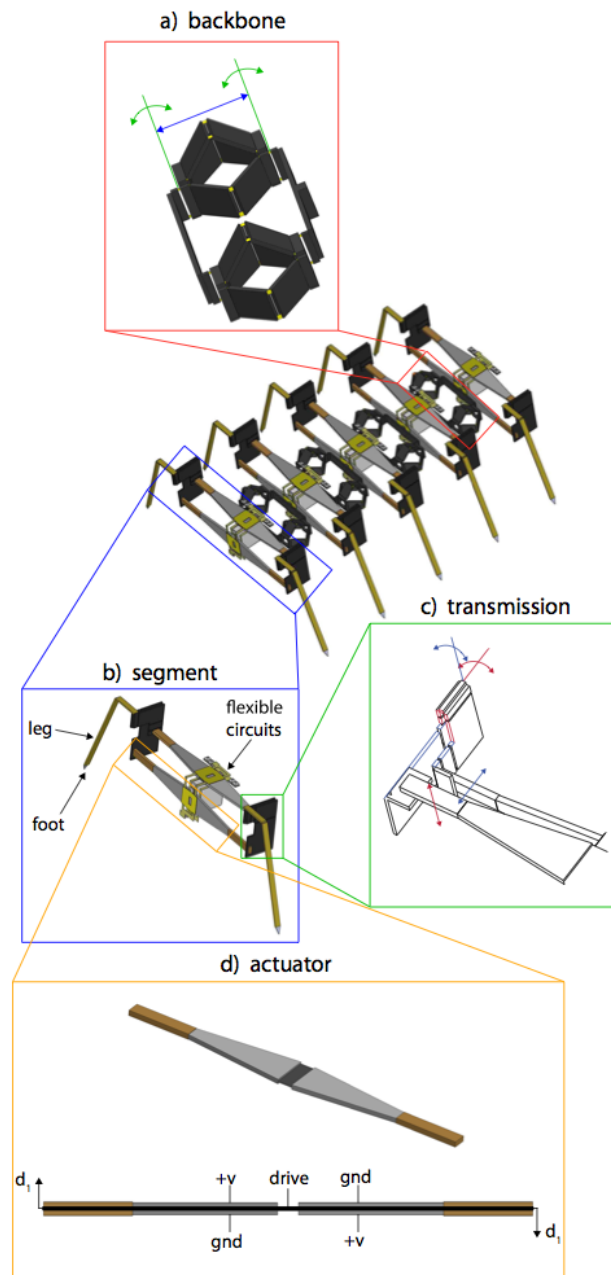


Fig. 2. Rendering of 5-segment millirobot showing detail of the a) backbone, b) segments, c) transmission, and d) actuators.

motion. Due to the modular nature of the system equations, a simulation was created that allows the number of segments, and other relevant parameters, to be easily altered. The parameters for this millirobot are given in [7], chosen based on the effect of various design parameters on simulated locomotion. The final segment weight is 220 mg and measures 4 cm foot to foot, 1 cm long and 1 cm tall.

III. STRAIGHT-LINE GAITS

A. Simulation

In order to determine simple strategies for turning, the best nominal straight-line gaits had to be found as a function of the number of segments to understand the transitions

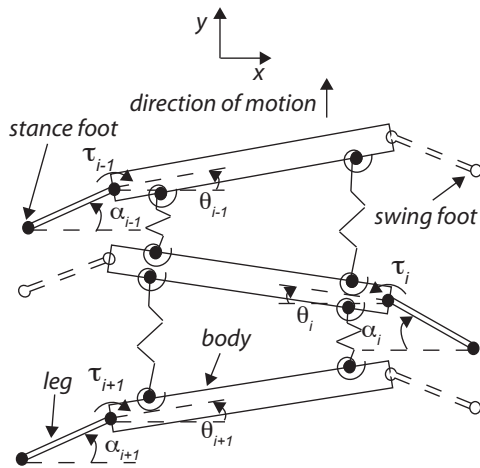


Fig. 3. Dynamic model of horizontal plane motion showing the DOF for each segment, θ and α , and the hip torque, τ .

between straight-line locomotion and turning. In [7], body undulations were shown to enhance locomotion for a 10-segment millirobot; however, due to the modular nature of the design, it was necessary to explore if this trend could be expanded to encompass millirobots with various numbers of segments.

Straight-line locomotion is parameterized by the following:

- 1) bias voltage, $+V$
- 2) frequency, f
- 3) phase between segments, ϕ
- 4) ramp rate of the trapezoidal drive signals

To determine the best straight-line gaits as a function of number of segments in simulation, the phase of the stance change between segments was varied while applying a constant torque at the hip joint of each segment. This was done for a range of frequencies (1-20 Hz) and a variety of millirobot sizes (3-25 segments). It was found, in general, that the optimal phase for a myriapod with n segments is $\frac{2\pi}{n-1}$ radians for maximizing speed and minimizing cost of transport. This is the smallest phase between segments that still allows the groups of stance legs that form along the length of the body to result in a tripod, maintaining static stability in the horizontal plane. Having three groups of legs is also very similar to undulatory centipede gaits found in nature [6]. In both nature and this millirobot, the body curves around the groups of stance legs, increasing step size. This is illustrated in the frames of motion from a simulation for a 7-segment millirobot in Fig. 4.

The speeds of the millirobot with different numbers of segments are plotted for a representative frequency of 10 Hz in Fig. 5 using the optimal phases of $\frac{2\pi}{n-1}$ radians. The alternating gait, or a phase of 180 degrees between segments, results in the slowest speeds across the range of segment numbers as well as the highest cost of transport defined as the energy required per distance per mass. This gait is generally used by rigid-body hexapods, but here, causes body

oscillations that reduce step-size and waste energy. Since this is the only phase a 3-segment centipede robot can use with contralaterally coupled legs while still maintaining static stability, this body morphology may not be the ideal choice for hexapods. There is a general upward trend in absolute speeds as the number of segments increases and the phase between segments decreases. As the phase between segments decreases, the amount of positive body rotation of each segment at the time of stance change increases, amplifying the severity of body undulations. Adding additional segments allows the phase to be decreased while still having a tripod of stability, allowing for millirobots with more segments to have larger undulations and faster gaits. These results predict that even for millirobots with only 8 legs, it is still possible to have locomotion-enhancing body undulations.

While the absolute speed increases, the speed relative to the body length decreases as shown in Fig. 6 over a range of frequencies for the four millirobot sizes that will be used in the experiments. In each case, the optimal undulatory gait is a better choice than the alternating gait. An additional undulatory gait was plotted for 8-segments to show that the undulatory gait with the smallest phase ($\frac{2\pi}{n-1}$ radians) causes more positive body rotation than other undulatory gaits, in this case, a phase of 90 degrees. For a fixed payload, such as onboard sensors, there could be a larger increase in absolute speeds as number of segments increases and phase of the drive signal decreases.

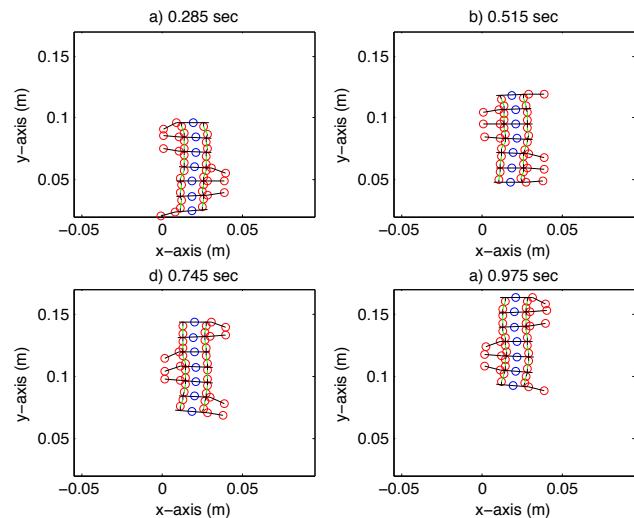


Fig. 4. Frames of motion from simulation showing body undulations at 5 Hz in a 7-segment millirobot, with stance legs and body segment plotted in black, stance feet and other rotational joints shown in red, sarrus linkages plotted in green, and the center of mass of each segment in blue.

B. Experimental Results

To verify the simulation results, the optimal undulatory gaits ($\frac{2\pi}{n-1}$ radians) and alternating gaits were tested on 5-8 segment millirobots for 1-10 Hz. An external power supply and high voltage amplifier, controlled by Matlab and an xPC target system (Mathworks) were used to drive the millirobot. The average speed of two trials for each gait at

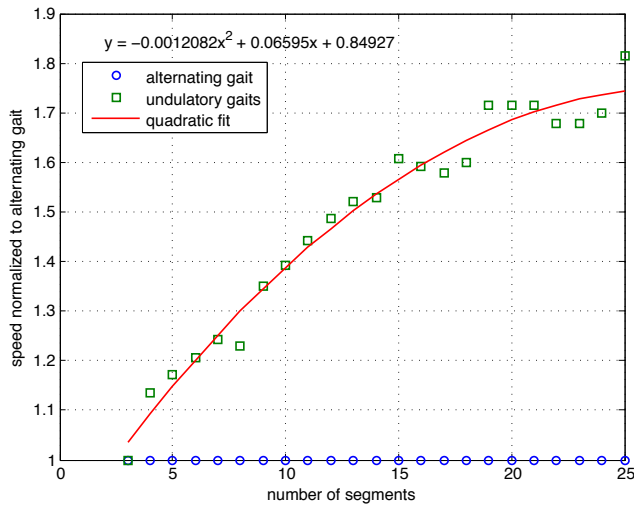


Fig. 5. Speed as a function of number of segments for alternating and optimal undulatory gaits at 10 Hz normalized to alternating gait speed.

each frequency are plotted in Fig. 7. This frequency range was chosen because above 10 Hz, there is a tendency for feet to slip with respect to ground, which causes losses and variations from the dynamic model. As can be seen, the optimal undulatory gaits result in faster straight-line locomotion over the entire frequency range for a variety of millirobots with differing numbers of segments compared to the alternating gait. Similar to the simulation results, frequencies between 4-8 Hz show the largest improvement over the alternating gaits. This is due to the negative body rotation for the alternating gait being at its maximum as the stance changes before it springs forward to zero body rotation, or no increase in step size. The benefit of having each segment be offset by a certain phase from each adjacent segment is that it simplifies the components necessary for onboard control. Upon generating the control signal for the first segment, each segment merely needs to phase shift that signal. This was also the motivation for the simple technique used for turning in Sec. IV as additional electronic components onboard can be costly for a robot at this scale. The alternating and optimal undulatory gaits are shown for a 6-segment millirobot in the Supplementary Video.

While the optimal undulatory gait for each length millirobot was generally an improvement over the alternating gait, there was not a noticeable increase in absolute speed as segment number increased. This could be due to slight differences between the model and actual millirobot, such as feet slipping, external wiring, or unmodeled flexure losses; however, the simulation was able to predict an improvement seen by the passive body undulations as compared to the alternating gait.

Due to the brittle nature of the piezoelectric actuators, instead of using a pure square wave to switch the torque when controlling opposite legs on the same segment, it is necessary to ramp the voltage up to the maximum value. It was found, both in simulation and experimentally, that the undulations become more pronounced as the ramp rate

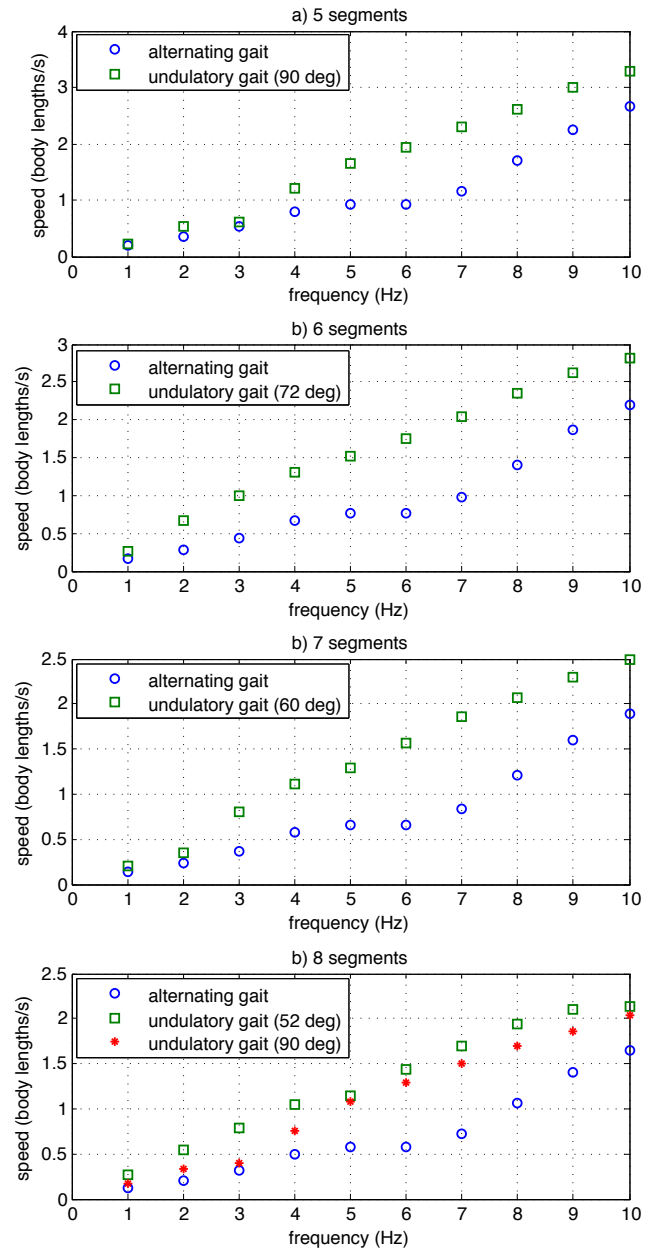


Fig. 6. Simulated average speeds for alternating and optimal undulatory gaits from 1-10 Hz for a) 5 segments b) 6 segments c) 7 segments and d) 8 segments.

is increased, approaching a constant hip torque. In these experiments, a ramp rate of 10 kV/s was used, although for the turning scheme chosen and described in Sec. IV, a frequency dependent ramp rate worked best. The transition between straight-line locomotion and turning could involve altering the ramp rate, or the ramp rate could remain constant and a slight decrease in body undulations could be chosen to reduce the complexity of the control strategy.

IV. TURNING GAITS

A. Simulation

The goal for establishing a turning gait was to find a simple method that did not involve introducing additional

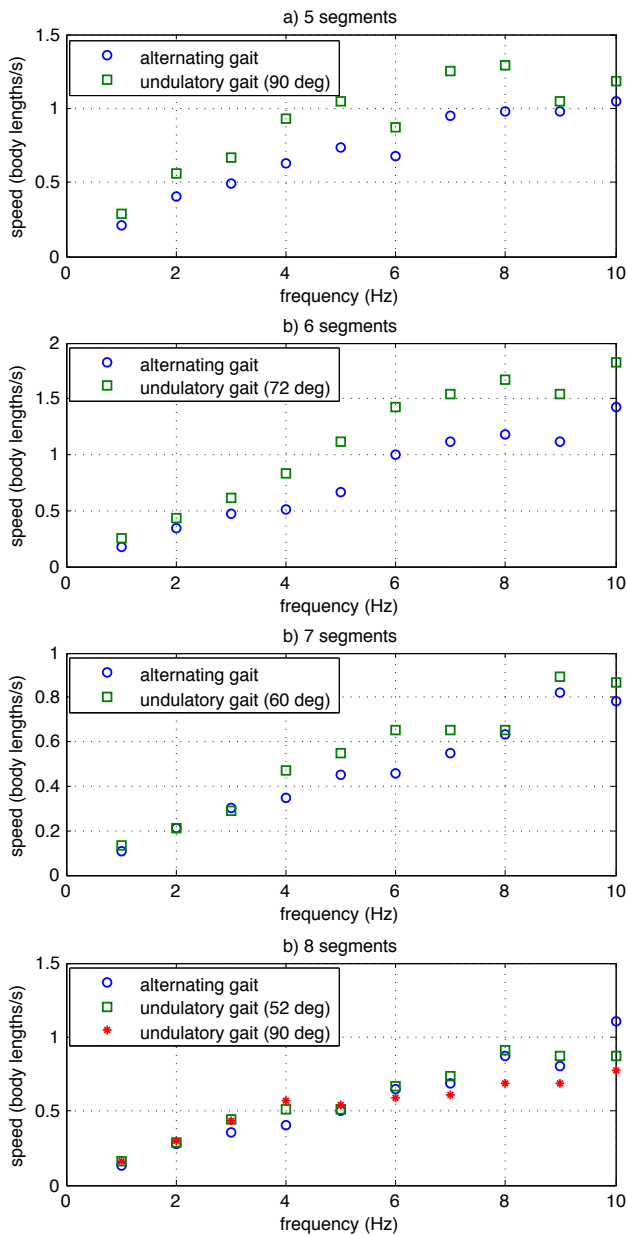


Fig. 7. Experimental average speeds for alternating and optimal undulatory gaits from 1-10 Hz for a) 5 segments b) 6 segments c) 7 segments and d) 8 segments.

actuation, is easily extended to a robot with any number of segments, and can transition between turning and the nominal undulatory gaits described in Sec. III. To do this, it was necessary to use the drive signals to cause an asymmetry in the gait of the robot and perturb it from its straight-line locomotion. The difficulty in this comes from the legs being coupled across the body, with one leg being placed on the ground as the opposite is being lifted and the torque applied to the stance leg affecting the touchdown angle of the swing leg.

The simulation was unable to give an accurate representation for turning due to the high forces on the feet causing them to no longer act as perfect pin joints, but was used to gauge if two strategies would cause any asymmetries in

the gait. The first strategy involved applying a larger torque to the stance leg on one side of the body as compared to the opposite leg by biasing the drive signal voltage. This method showed very little perturbation from the nominal straight-line gait due to the coupling between legs. The leg being subjected to a smaller torque on one side of the body rotated less. However, due to the coupling between legs, the leg subjected to the larger torque had a smaller initial touchdown angle, and, therefore, also experienced less rotation. A second method for turning involves changing the duty-cycle for the stance control actuator, causing the legs on one side of the body to remain on the ground longer than the legs on the opposite side and, therefore, have a larger stride. In simulation, this proved to cause a larger asymmetry in the gait than biasing the torque. Using this method, contralateral legs would be subject to the same maximum torque as for straight-line locomotion, just for different lengths of time.

B. Experimental Results

To implement turning experimentally, a Matlab controller was created based on the parameterization of the turning strategy with the ability to smoothly transition between turning and straight-line locomotion. Turning via altering the time opposite legs are on the ground can be parameterized by the following:

- 1) duty-cycle for the stance and swing control signals, t_d
- 2) the ramp rate for the trapezoidal drive signals

To simplify the controller, the frequency and phase between segments will remain constant for straight-line and turning locomotion. The duty-cycle must be chosen to cause an asymmetry in the drive signal, but still maintain static stability in the vertical plane. A duty-cycle of 50 percent represents a symmetric drive signal. For example, a duty cycle of 100 percent would mean all stance legs are on one side of the body (with 0 percent meaning all stance legs are on the opposite side of the body), which is not statically stable. The minimum duty-cycle that can be used while still maintaining static stability is dependent on the number of segments and phase between segments. In the experiments performed here, a duty-cycle of 25 percent for left turns (or 75 percent for right turns) was used, as it was compatible with the 5-8 segment robots and their nominal gaits. Note that this strategy would not work for hexapods as static stability would not be maintained for any duty-cycle other than 50 percent.

While a fast ramp rate of 10 kV/s works best when changing the torque applied to the swing DOF for straight-line locomotion, a frequency dependent swing drive signal ramp rate works better for turning. It was found, by altering the ramp rate experimentally, that the ramp rate for the swing drive signal that causes the highest turning rate is $0.8f$ kV/s for a bias voltage of 200 V and duty-cycle offset of 25 percent. The straight-line and turning drive signals are shown in Fig. 8. By having a ramp rate of $0.8f$ kV/s for turning, the drive signal is ramped slowly enough to just hit the voltage limit, or maximum torque, for the leg that is on the ground for the shorter time span before the stance is

switched. This means the maximum torque on that hip is applied for the shortest amount of time while still allowing the opposite leg to fully reset in preparation for the next step due to the coupling of the legs. The ramp rate of the stance control always remains at 10 kV/s to switch stance as close to instantaneously as possible.

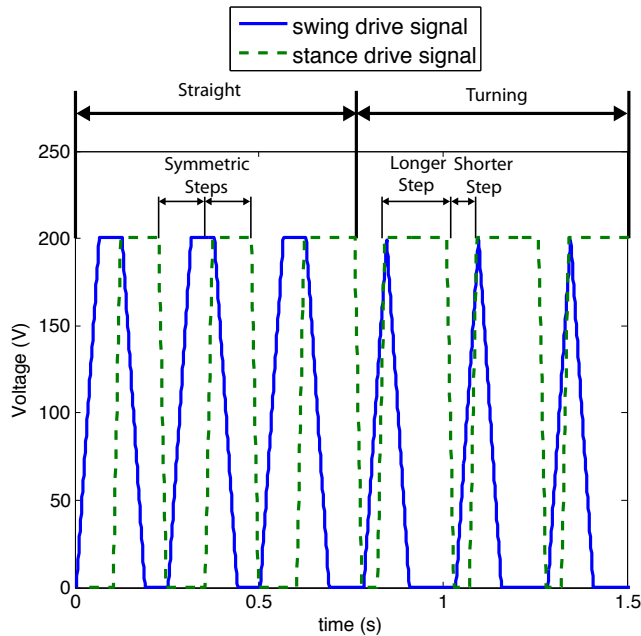


Fig. 8. Drive signals for stance and swing control for straight-line and turning motions.

Another choice had to be made as to whether all legs would be involved in turning or if turning could be achieved by merely altering the gait of the first segment. It was found experimentally that only altering the duty-cycle of the first segment creates large reaction forces on the stance feet of the first segment, causing them to slip as the remaining segments push the first segment forward. This does not result in turning. Additionally, requiring all segments to be involved in turning not only distributes the asymmetry along the length of the millirobot, but it also allows each segments' drive signal to be the same as the first segment, merely offset by a constant phase. Each segment begins the turn at a time of $\frac{\phi}{2\pi f}$ seconds (where ϕ is in radians) after the adjacent segment.

To demonstrate turning for robots with an arbitrary number of segments, the method described here was implemented in millirobots with 5, 6, 7, and 8 segments. Each of the four millirobots were run at 4 Hz. Five cases were tested: straight-line locomotion using the optimal undulatory gait, walking straight for 10 steps then turning left or right for the remainder of the time, and walking straight for 10 steps followed by turning left or right for 16 steps (2 seconds) then walking straight for the remainder of the time. Each trial was repeated 5 times to test for consistency for a total of 25 runs per robot. Representative plots of the center of mass (COM) are shown for 5- and 8-segment millirobots in

Fig. 9, although similar results were also found for 6- and 7-segment millirobots, demonstrating the effectiveness of this turning method for a modular millirobot. The orientation of the millirobot is illustrated by the images of the millirobot as it appears at the end of each of the five different experiments. As can be seen in Fig. 9, when changing the duty-cycle of the drive signal, the millirobot is able to consistently perform left and right turns, as well as alter the severity of turns by changing the amount of time spent turning. This also shows that it can easily transition between straight-line locomotion to turning and back again. Sample videos for turning in a 5-segment millirobot can be found in the Supplementary Video.

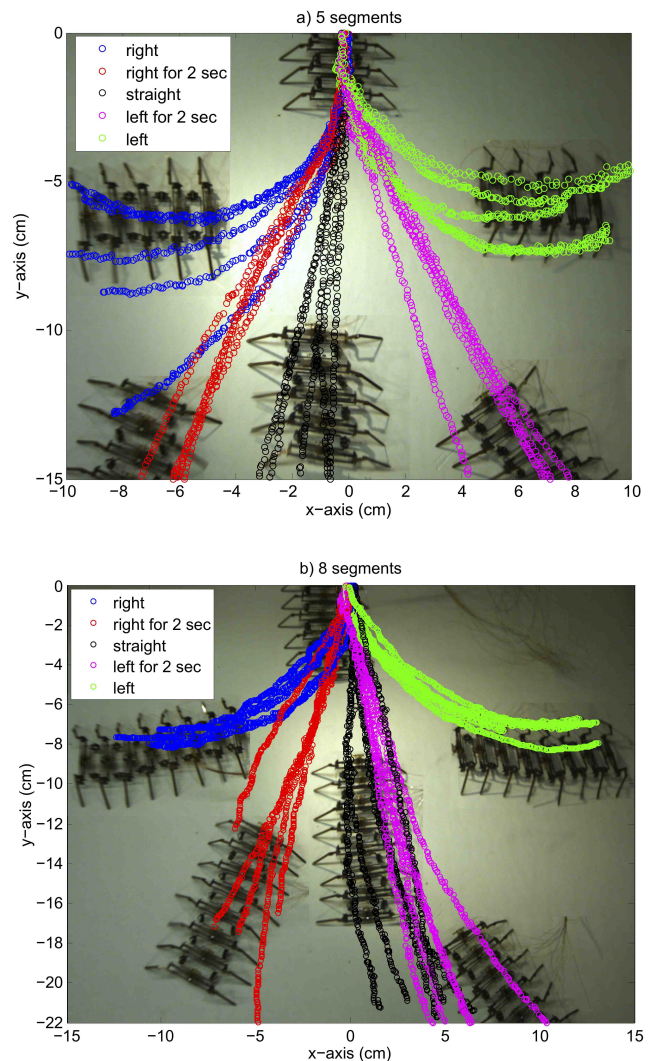


Fig. 9. Center of mass tracking for turning and straight-line gaits for a) 5-segment and b) 8-segment millirobots at 4 Hz. Sample videos of turning can be found in the Supplementary Video.

For each of the above trials for 5-8 segment millirobots, the average turning rate and turning radius were calculated and are shown in Fig. 10. There was no obvious correlation between turning rate or radius and number of segments. The turning radii were all in the neighborhood of one body length.

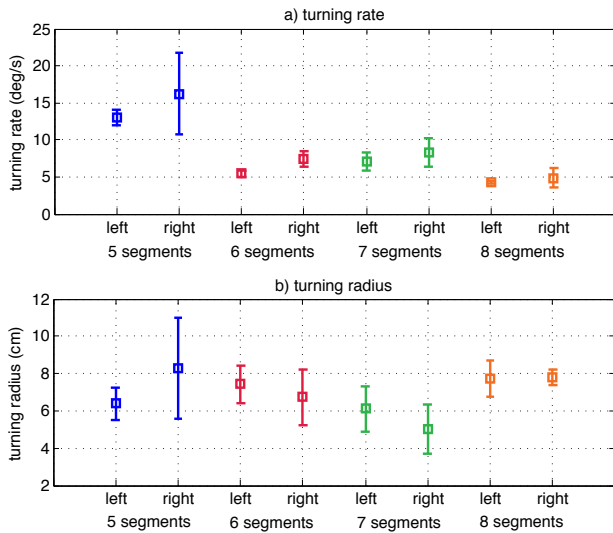


Fig. 10. a) Turning rate and b) turning radius averaged over 5 trials for millirobots with 5-8 segments. Error bars represent one standard deviation.

To demonstrate that this turning strategy works over a range of frequencies, it was tested on the 6-segment millirobot between 1-10 Hz, using a drive signal ramp rate of $0.8f$ kV/s and a 25 percent offset in duty-cycle. The turning rates and radii are plotted in Fig. 11. As can be seen in Fig. 11(a), the turning rates for this 6-segment millirobot increase to a maximum of 8 deg/s at 10 Hz. The increase in turning radius with frequency is less consistent, but higher frequencies tend to have a larger turning radius.

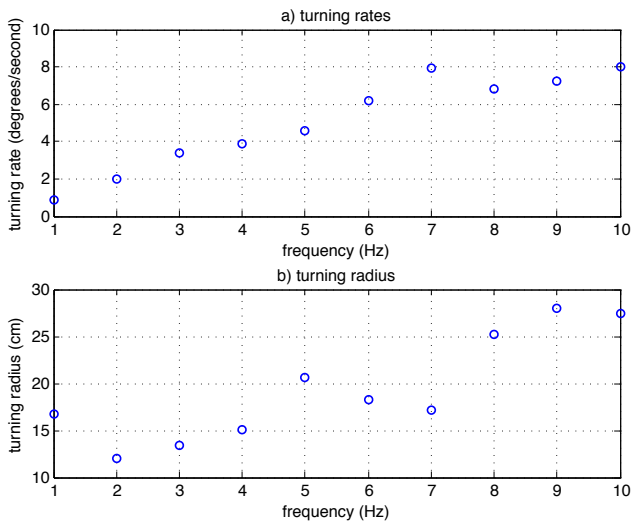


Fig. 11. a) Turning rate and b) turning radius as a function of frequency for a 6-segment millirobot.

Consecutive turns were performed using a 6-segment millirobot over a range of frequencies. The COM tracking with three video frames of the robot at different positions during the maneuver from a trial at 4 Hz is shown in Fig. 12. A trial at 10 Hz is included in the Supplementary Video.

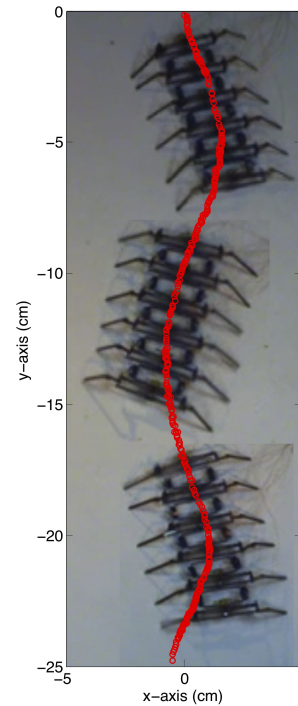


Fig. 12. Center of mass tracking of 6-segment millirobot performing consecutive turns at 4 Hz.

V. CONCLUSIONS AND FUTURE WORK

Locomotion of a modular, centipede-inspired millirobot with a passive flexible backbone and underactuated design was presented. Optimal undulatory gaits were demonstrated in simulation and experimentally for millirobots with 5-8 segments, and these gaits were found to result in faster locomotive speeds than the alternating gait typically used in hexapods. The optimal undulations resulting at a phase of $\frac{2\pi}{n-1}$ radians are similar to those found in biological centipedes with the body rotating about three clumps of legs distributed along the length of the body and increasing step size. A simple turning strategy which alters the duty-cycle of the stance control was developed and implemented in the millirobot. This turning strategy worked for millirobots with varying numbers of segments and transitions between straight-line locomotion and turning were demonstrated.

Future work includes improving the backbone design of the millirobot. While the passive backbone successfully creates locomotion-enhancing undulations using the natural system dynamics, the off-axis compliance causes the leg lifting height to be reduced for the optimal undulatory gait as the number of segments increases due to more segments in a row having the same stance leg. Additional joints will also be added to allow the millirobots to morph to a variety of surfaces.

The millirobot shown here was controlled using off-board electronics. On-board electronics similar to those in [3] are being designed for this millirobot. These straight-line and turning strategies simplify the controllers necessary for

coordinated motion of the millirobot as each drive signal is merely a phase shifted version from the first segment.

A hypothesized advantage of a myriapod millirobot is robustness to leg failures. With many legs, if one is lost, locomotion should still be possible. Qualitative observations have shown that even when a 5-segment version of this millirobot loses a leg, it is still able to locomote. This will be further studied in an extended version of the simulation described here and in [7] as well as experimentally.

The biologically-inspired design and locomotion of this millirobot will allow us to study biological centipede locomotion and understand how body flexibility and many legs can be implemented into millirobots for efficient locomotion.

VI. ACKNOWLEDGMENTS

This work was partially supported by the Wyss Institute for Biologically Inspired Engineering (Harvard University) and the National Science Foundation (under award number IIS-0811571). Any opinions, findings and conclusions or recommendations expressed in this material are those of the authors and do not necessarily reflect those of the National Science Foundation. This research was also made with Government support under and awarded by DoD, Air Force Office of Scientific Research, National Defense Science and Engineering Graduate (NDSEG) Fellowship, 32 CFR 168a.

REFERENCES

- [1] A. Hoover, S. Burden, X. Fu, S. Sastry, and R. Fearing, "Bio-inspired design and dynamic maneuverability of a minimally actuated six-legged robot," in *IEEE International Conference on Biomedical Robotics and Biomechanics*, 2010.
- [2] P. Birkmeyer, K. Peterson, and R. Fearing, "DASH: A Dynamic 16g Hexapedal Robot," *Proc. IEEE/RSJ International Conference on Intelligent Robots and Systems*, 2009.
- [3] A. Baisch, C. Heimlich, M. Karpelson, and R. Wood, "HAMR3: An Autonomous 1.7g Ambulatory Robot," *Proc. IEEE/RSJ International Conference on Intelligent Robots and Systems*, 2011.
- [4] G. Edgecombe and G. Giribet, "Evolutionary biology of centipedes (myriapoda: Chilopoda)," *Annu. Rev. Entomol.*, vol. 52, pp. 151–170, 2007.
- [5] S. Manton and M. Harding, "The evolution of Arthropodan locomotory mechanisms - Part 3. The locomotion of the Chilopoda and Pauropoda," *Journal of the Linnean Society of London, Zoology*, vol. 42, no. 284, pp. 118–167, 1952.
- [6] B. Anderson, J. Shultz, and B. Jayne, "Axial kinematics and muscle activity during terrestrial locomotion of the centipede *Scolopendra heros*," *Journal of Experimental Biology*, vol. 198, no. 5, pp. 1185–1195, 1995.
- [7] K. Hoffman and R. Wood, "Passive Undulatory Gaits Enhance Walking In A Myriapod Millirobot," *Proc. IEEE/RSJ International Conference on Intelligent Robots and Systems*, 2011.
- [8] Y. Zhang, M. Yim, C. Eldershaw, D. Duff, and K. Roufas, "Phase automata: a programming model of locomotion gaits for scalable chain-type modular robots," vol. 3, pp. 2442–2447, 2003.
- [9] B. Jimenez and A. Ikspeert, "Centipede robot locomotion," Master's thesis, Ecole Polytechnique Federale de Lausanne, 2007.
- [10] M. Sfakiotakis and D. Tsakiris, "Undulatory and pedundulatory robotic locomotion via direct and retrograde body waves," *IEEE International Conference on Robotics and Automation*, pp. 3457–3463, 2009.
- [11] J. Sastra, W. Bernal-Heredia, J. Clark, and M. Yim, "A biologically-inspired dynamic legged locomotion with a modular reconfigurable robot," *Proc. of DSCC ASME Dynamic Systems and Control Conference*, 2008.
- [12] D. Koh, J. Yang, and S. Kim, "Centipede robot for uneven terrain exploration: Design and experiment of the flexible biomimetic robot mechanism," *3rd IEEE RAS and EMBS International Conference on Biomedical Robotics and Biomechanics*, 2010.
- [13] J. Whitney, P. Sreetharan, K. Ma, and R. Wood, "Pop-up book mems," *Journal of Micromechanics and Microengineering*, vol. 21, no. 11, pp. 115 021–115 027, 2011.